# Kinetic Analysis of the Unfolding and Refolding of Ribonuclease T1 by a Stopped-Flow Double-Mixing Technique[†,‡]

Lorenz M. Mayr,[§,||] Christian Odefey,[§] Mike Schutkowski,[⊥] and Franz X. Schmid*[,§]

*Laboratorium für Biochemie, Universität Bayreuth, D-95440 Bayreuth, Germany, and Max-Planck-Gesellschaft, Arbeitsgruppe "Enzymologie der Peptidbindung", Weinbergweg 16a, D-06120 Halle/Saale, Germany*

*Received December 21, 1995; Revised Manuscript Received February 21, 1996*[⊗]

ABSTRACT: Often protein folding reactions show complex kinetics, because multiple unfolded species are present, which refold simultaneously. After conformational unfolding, these species are formed by the slow *cis*/*trans* equilibrations at Xaa−Pro peptide bonds. To dissect the roles of individual prolines for unfolding and refolding, we used ribonuclease T1, a protein with two *cis* prolyl peptide bonds, preceding Pro39 and Pro55, and two variants with substitutions at these positions. A stopped-flow double-mixing technique was employed (i) to measure the rates of the individual prolyl isomerizations in the unfolded proteins and (ii) to study the refolding of transient species that are not well populated at equilibrium. In particular, the elusive species with correct prolyl isomers could be produced by short unfolding pulses, and its refolding kinetics could be measured. The two isomerizations in unfolded ribonuclease T1 could be assigned to Pro39 and Pro55, because they occurred with almost identical rates in the wild-type protein, in the single-*cis* proline variants, and in tetrapeptide-4-nitroanilides, which contained prolines in the same sequential context as Pro39 and Pro55 of ribonuclease T1. The direct refolding reaction of the unfolded molecules with correct prolyl isomers shows a time constant of 180 ms (at 25 °C, pH 4.6). This reaction is almost unaffected by the proline substitutions. It depends nonlinearly on temperature with a maximum near 25 °C, which suggests that the activated state for this reaction resembles the native rather than the unfolded state in heat capacity. The formation of a transient intermediate with incorrect prolyl isomers could be studied as well. Surprisingly, this reaction is only about 5-fold slower than direct folding, and it is also accompanied by a strong decrease in the apparent heat capacity.

The *cis*/*trans* isomerizations of prolyl peptide bonds are slow steps in protein folding both *in vitro* and *in vivo* (Brandts *et al.*, 1975; Schmid & Baldwin, 1978; Schmid, 1993; Schmid *et al.*, 1993; Engel & Prockop, 1991). *cis* ⇌ *trans* equilibria are established at the prolines[1] in an unfolded polypeptide chain, and, as a consequence, denatured proteins are usually heterogeneous mixtures of species which follow different pathways for refolding. Only molecules with native-like prolines[1] can refold directly in a rapid reaction. Molecules with non-native incorrect prolines refold slowly, in reactions that are limited in rate by the *cis*/*trans* isomerizations at these prolines. Proline-limited folding reactions are catalyzed *in vitro* and *in vivo* by peptidyl prolyl *cis*/*trans* isomerases (Fischer *et al.*, 1984; Lang *et al.*, 1987; Bächinger, 1987; Lin *et al.*, 1988; Schmid, 1993; Schmid *et al.*, 1993; Steinmann *et al.*, 1991; Rassow *et al.*, 1995; Matouschek *et al.*, 1995).

Here we use ribonuclease T1 (RNase T1)[2] to dissect the roles of individual proline residues in the folding mechanism. RNase T1 is a small protein of 104 residues (Heinemann & Saenger, 1982; Martinez-Oyanedel *et al.*, 1991; Pace *et al.*, 1991), which has served as a model protein for the investigation of proline-limited folding reactions (Kiefhaber *et al.*, 1990a,b,c; Mayr *et al.*, 1993; Mücke & Schmid, 1994b). It contains four prolyl peptide bonds: the bonds preceding Pro60 and Pro73 are *trans* in the native protein; those preceding Pro39 and Pro55 are *cis* (Martinez-Oyanedel *et al.*, 1991). Pro39 is near the active site in the protein interior, and the *cis* conformation of the 38−39 peptide bond is conserved after the replacement of Pro39 by an alanine (Mayr & Schmid, 1993b; Mayr *et al.*, 1994; Odefey *et al.*, 1995). The other *cis* proline[1] at position 55 is in an external loop and maintains few contacts to other regions of the RNase T1 molecule. After the replacement of Ser54-Pro55 by

[†] This work was supported by grants from the Deutsche Forschungsgemeinschaft and the Fonds der Chemischen Industrie.

[‡] This paper is dedicated to Prof. Dr. Max Herberhold on the occasion of his 60th birthday.

* To whom correspondence should be addressed. Telephone: ++49 921 553660. Fax: ++49 921 553661.

[§] Universität Bayreuth.

[||] Present address: Bayer AG, Zentrale Forschung, Forschung Molekularbiologie, D-51368 Leverkusen, Germany.

[⊥] Max-Planck-Gesellschaft.

[⊗] Abstract published in *Advance ACS Abstracts,* April 1, 1996.

[1] To facilitate reading, we use the terms "*cis* proline" and "*trans* proline" for proline residues that are preceded by a *cis* or a *trans* peptide bond, respectively, in the *folded* protein and "isomerization of ProX" for the isomerization of the prolyl peptide bond preceding ProX. Folding reactions that involve Xaa−Pro isomerizations as rate-limiting steps are denoted as "proline-limited" reactions; the (usually) rapid folding of the unfolded molecules which have the Xaa−Pro peptide bond in the same conformation as the native protein is denoted as the "direct" folding reaction.

[2] Abbreviations: RNase T1, ribonuclease T1; S54G/P55N-RNase T1, a variant of RNase T1 with the substitutions Ser54→Gly and Pro55→Asn; P39A-RNase-T1, a variant of ribonuclease T1 with the substitution Pro39→Ala; N, native protein; $U^{39c}_{55c}$, $U^{39t}_{55c}$, $U^{39c}_{55t}$, and $U^{39t}_{55t}$, unfolded forms of RNase T1 with Pro39 and Pro55 in the *cis* (*c*) or *trans* (*t*) conformations; $I^{39t}_{55c}$, $I^{39c}_{55t}$, and $I^{39t}_{55t}$, folding intermediates with Pro39 and Pro55 in the *cis* (*c*) or *trans* (*t*) conformations; GdmCl, guanidinium chloride; $\tau$, time constant of a reaction ($\tau$ is the reciprocal of the measured or apparent rate constant); $k_{ij}$, microscopic rate constant.

S0006-2960(95)03035-2 CCC: $12.00 

Scheme 1: Kinetic Model for the Unfolding and Isomerization of RNase T1[a]

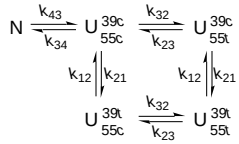

[a] This model is valid for unfolding only. The superscript and the subscript indicate the isomeric states of prolines 39 and 55, respectively, in the correct, native-like *cis* (*c*) and in the incorrect, non-native *trans* (*t*) isomeric states. As an example, $U_{55c}^{39t}$ is an unfolded species with Pro39 in the incorrect *trans* and Pro55 in the correct *cis* state. In the denatured protein, the two isomerizations are independent of each other; therefore, the scheme is symmetric with identical rate constants in the horizontal and vertical directions, respectively.

Gly54-Asn55, this peptide bond is *trans* in folded S54G/P55N-RNase T1 (Kiefhaber *et al.*, 1990; Hinrichs *et al.*, unpublished results).

The equilibrium unfolding transitions of RNase T1 closely follow the two-state approximation (Pace & Laurents, 1989; Kiefhaber *et al.*, 1990; Hu *et al.*, 1992; Yu *et al.*, 1994), but the unfolding and refolding kinetics are complex processes in the presence as well as in the absence of the two disulfide bonds. The conformational unfolding reaction is followed by slow prolyl isomerizations of the denatured protein chains, and at equilibrium at least four different unfolded species coexist, three of which contain incorrect *trans* isomers of Pro39 and/or Pro55 (Kiefhaber *et al.*, 1990b, 1992; Mücke & Schmid, 1994a,b; Mayr *et al.*, 1994).

A kinetic mechanism for the unfolding of RNase T1 is proposed in Scheme 1. The conformational unfolding reaction ($N \rightarrow U_{55c}^{39c}$) is followed by slow isomerizations at Pro39 and Pro55. Both are *cis* in N and in $U_{55c}^{39c}$, but isomerize largely to the more favorable *trans* state in the unfolded protein. As a consequence, only 2−4% of all unfolded molecules remain in the $U_{55c}^{39c}$ state with P39 and P55 in the correct *cis* state, and the species with two incorrect isomers ($U_{55t}^{39t}$) predominates at equilibrium. The species with single incorrect isomers ($U_{55c}^{39t}$ and $U_{55t}^{39c}$) are populated to approximately 10−20% each. The two *trans* prolines do not contribute significantly to the folding of RNase T1 (L. M. Mayr, unpublished observations) and are not accounted for in Scheme 1.

Individual refolding paths originate from the different unfolded species in Scheme 1, and the kinetic model for the refolding of RNase T1 under strongly native conditions (Kiefhaber *et al.*, 1990b) is shown in Scheme 2. The two slow-folding species with one incorrect prolyl isomer each ($U_{55c}^{39t}$ and $U_{55t}^{39c}$) and the species with both prolines in the incorrect isomeric state ($U_{55t}^{39t}$) can regain rapidly most of their secondary structure in the milliseconds range (the $U_i \rightarrow I_i$ steps, Scheme 2) (Kiefhaber *et al.*, 1992). Subsequently, slow folding steps follow that involve the isomerizations of the incorrect prolyl isomers. A peculiar feature of the folding model in Scheme 2 is that the major unfolded species with two incorrect isomers can enter two alternative folding pathways (the upper or the lower pathway in Scheme 2), depending upon which isomerization occurs first. The distribution of refolding molecules on these two pathways is determined by the relative rates of the *trans* → *cis* isomerizations of Pro39 and Pro55 at the stage of the intermediate $I_{55t}^{39t}$.

Scheme 2: Kinetic Model for the Slow Refolding of RNase T1 under Strongly Native Conditions[a]

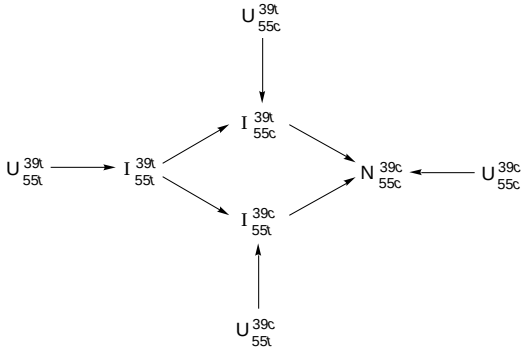

[a] U stands for unfolded species, I for intermediates of refolding, and N is the native protein. The superscript and the subscript indicate the isomeric states of prolines 39 and 55, respectively, in the correct *cis* (*c*) and the incorrect *trans* (*t*) isomeric states.

These kinetic models are supported by experimental data on the slow folding of wild-type RNase T1 and of variants where the *cis* prolines were replaced by other amino acids (Kiefhaber *et al.*, 1990c; Mayr *et al.*, 1993a,b). The mechanism in Scheme 2 is complex, but clearly a simplification. It is valid only under strongly native conditions, and contributions from minor species (e.g., with incorrect isomers at the *trans* prolines 60 and 73) are not included.

The fast refolding reaction ($U_{55c}^{39c} \rightarrow N$) could not yet be measured because at equilibrium only 2−4% of all unfolded RNase T1 molecules are in the $U_{55c}^{39c}$ state. Its existence was inferred, however, from the formation of a small amount of native RNase T1 molecules early in refolding, within the dead time of manual mixing (Kiefhaber *et al.*, 1990b). Similarly, little is known about the rate of formation of the partially-folded intermediates with incorrect prolyl isomers ($I_{55t}^{39t}$, $I_{55t}^{39c}$, and $I_{55c}^{39t}$ in Scheme 2). Their existence was inferred from the rapid regain of the amide circular dichroism within 20 ms and from the rapid protection of amide protons from exchange with the solvent (Kiefhaber *et al.*, 1990b, 1992a; Mullins *et al.*, 1993).

The sequential nature of unfolding ($N \rightarrow U_{55c}^{39c}$) and prolyl isomerizations (cf. Scheme 1) provides a means for investigating the direct $U_{55c}^{39c} \rightarrow N$ folding reaction, even though $U_{55c}^{39c}$ is not significantly populated at equilibrium. $U_{55c}^{39c}$ can be produced transiently at a high concentration by a short unfolding pulse under conditions, where the $N \rightarrow U_{55c}^{39c}$ unfolding reaction is much faster than the subsequent prolyl isomerizations (Brandts *et al.*, 1975; Schmid, 1986; Houry *et al.*, 1994). To this end, we first searched for such unfolding conditions and then used a stopped-flow double-mixing technique to accumulate $U_{55c}^{39c}$ at a high concentration in the first step and then measure its refolding in the second step. In addition, the duration of the unfolding step was varied to monitor the concentrations of all species of the wild-type protein in Scheme 1 as a function of time. Similar experiments were carried out with the S54G/P55N variant (this work) and on the P39A variant (Odefey *et al.*, 1995) to identify the contributions of the individual *cis* prolines to the unfolding and refolding kinetics.

## MATERIALS AND METHODS

*Materials.* Wild-type RNase T1 and the S54G/P55N variant were purified as described (Mayr & Schmid, 1993b)

from *Escherichia coli* cells transformed with a plasmid carrying a chemically synthesized gene (Quaas *et al.*, 1988). GdmCl (ultrapure) was from Schwarz/Mann (Orangeburg, NJ). All other chemicals were from Merck (Darmstadt, Germany). The concentrations of RNase T1 were determined spectrophotometrically using the absorption coefficient $A_{278}^{0.1\%} = 1.9$ of the wild-type protein (Takahashi *et al.*, 1970; Yu *et al.*, 1994). For optical measurements, a Hitachi F4010 fluorescence spectrometer and a Kontron Uvikon 860 spectophotometer were used.

*Stopped-Flow Double-Mixing Experiments.* All rapid double-mixing experiments were carried out using a DX.17MV double-mixing stopped-flow spectrometer from Applied Photophysics (Leatherhead, U.K.). The protein samples were unfolded by the first mixing and then, after a variable delay time, refolded by the second mixing. The time course of fast refolding after the second mixing was followed by the increase in integral tryptophan fluorescence above 300 nm. Excitation was at 278 nm (10 nm bandwidth). The path length of the observation chamber was 0.2 cm. A 10 mM aqueous solution of cytidine 2′-phosphate in a 0.2-cm cuvette was inserted between the observation chamber and the emission photomultiplier to absorb scattered light from the excitation beam. The photomultiplier voltage was set at 800 V in all experiments. The dead time between the start of the reaction and the begin of data collection was determined to be 0.5 ± 0.3 ms by using the reaction between 2,6-dichlorophenolindophenol and L-ascorbate (Tonomura *et al.*, 1978).

In all experiments, 20 $\mu$L of native protein (36 $\mu$M in 0.01 M sodium acetate, pH 5.0) was diluted with 100 $\mu$L of 7.2 M GdmCl, 0.1 M glycine (pH 1.5), to give unfolding conditions of 6 $\mu$M protein in 0.083 M glycine hydrochloride, 6.0 M GdmCl (pH 1.6). Refolding in the second mixing step was induced after variable delay times by a further 6-fold dilution of the product of the first mixing step in the delay line with 0.1 M sodium acetate (pH 5.0) to give final folding conditions of 1 $\mu$M protein in 1.0 M GdmCl, 0.083 M sodium acetate (pH 4.6).

To test for the absence of mixing artifacts, the protein was replaced by 36 $\mu$M *N*-acetyltryptophanamide, and experiments as described above were performed. The emission of tryptophan decreased less than 3% within 1 s after the second mixing in these controls. The long-term stability was, however, limited, and the emission decreased by about 20% within 1 h. This decrease in intensity was correlated with the width of the excitation slit and is presumably caused by photodegradation.

All kinetic experiments were reproduced at least once. The individual refolding kinetics observed after the second mixing were analyzed as the sum of one or two exponential functions and a linear term, by using the software provided by Applied Photophysics. The linear term accounted for the small effect of photodecomposition and, after extended times of unfolding in the first step, for the onset of the slow refolding reactions.

*Calculation of the Rate Constants of Unfolding and Refolding.* The results of the double-mixing experiments give information on the mechanisms of both unfolding and refolding. The analysis of the refolding kinetics after the second mixing gives the rates of refolding of the various unfolded species which are present after a certain time of unfolding (i.e., the refolding mechanism). The variation of the amplitudes of refolding with unfolding time reflects the formation and the decay of the different unfolded species (i.e., the unfolding mechanism). As a consequence, unfolding and refolding are closely interrelated. Both consist of several folding and isomerization steps and are too complex for a rigorous kinetic treatment. Rather, we used the plausible mechanisms for unfolding and for refolding that were proposed earlier for the wild-type protein (Schemes 1 and 2) (Kiefhaber *et al.*, 1990b) and for the S54G/P55N variant (Kiefhaber *et al.*, 1990c; Mayr *et al.*, 1993a) to analyze the unfolding and refolding kinetics. Generally we assumed that the amplitude of a particular refolding reaction as measured by fluorescence is a linear function of the concentration of the species that it originates from.

The slow phases of the refolding of the wild-type protein and the S54G/P55N variant have been studied previously. They show time constants between 50 and 1000 s. In the stopped-flow experiments (which lasted for less than 6 s), the onset of these slow reactions was accounted for by including a linear term in the fit equation. The contributions of this term were generally small.

*Kinetics of Refolding of the Wild-Type Protein.* In all experiments, the fast refolding was fit to a sum of two exponential functions, and we assumed that the fastest phase (phase 1 with the time constant $\tau_1$) reflects the direct folding reaction $U_{55c}^{39c} \rightarrow N$ and the second fastest phase ($\tau_2$) reflects the formation of the intermediates $I_{55c}^{39t}$ and $I_{55t}^{39c}$ from the species $U_{55c}^{39t}$ and $U_{55t}^{39c}$, respectively (cf. Scheme 2).

The $U_{55c}^{39c} \rightarrow N$ reaction and the $U_{55t}^{39c} \rightarrow I_{55t}^{39c}$ reactions were assigned a specific change in fluorescence of $c_1$ (eq 5). When an individual fit parameter, $c_3$, was used for the specific change in fluorescence in the $U_{55t}^{39c} \rightarrow I_{55t}^{39c}$ reaction, values of $(0.95 \pm 0.10)c_1$ were observed for $c_3$. Therefore, $c_3$ was set equal to $c_1$, suggesting that $I_{55t}^{39c}$ shows a native-like fluorescence. The $U_{55c}^{39t} \rightarrow I_{55c}^{39t}$ reaction was assigned a specific fluorescence change of $c_2$.

*Kinetics of Unfolding and Isomerization of the Wild-Type Protein.* The dependences of the amplitudes of the refolding reactions 1 and 2 on the duration of unfolding were used to determine the rate constants of unfolding and prolyl isomerization based on the mechanism in Scheme 1. To evaluate this mechanism and to calculate the microscopic rate constants for unfolding ($k_{43}$), for Pro39 isomerization ($k_{23}$ and $k_{32}$), and for Pro55 isomerization ($k_{12}$ and $k_{21}$), a nonlinear least-squares fit of the experimental data to the unfolding mechanism (Scheme 1) was performed. For the fit, the program EASY-FIT (Schittkowski, 1993) was used. In this procedure, the differential eqs 1−5 are employed, which describe the dependence on unfolding time of the concentrations of the various species in Scheme 1. As outlined above, we assumed that phase 1 of the observed refolding kinetics originates from the $U_{55c}^{39c} \rightarrow N$ reaction, and that phase 2 originates from the $U_{55c}^{39t} \rightarrow I_{55c}^{39t}$ and the $U_{55t}^{39c} \rightarrow I_{55t}^{39c}$ reactions according to Scheme 2. $c_1$ is the fit parameter that describes the specific change in fluorescence during the $U_{55c}^{39c} \rightarrow N$ and the $U_{55t}^{39c} \rightarrow I_{55t}^{39c}$ reactions, and $c_2$ is the fit parameter for the specific fluorescence change during the $U_{55c}^{39t} \rightarrow I_{55c}^{39t}$ reaction. Fits, in which the $U_{55t}^{39t} \rightarrow I_{55t}^{39t}$ reaction was allowed to also contribute to phase 2 by including an additional term $c_3 U_{55t}^{39t}$ into eq 5, always resulted in values

for $c_3$ that were close to zero.

$$\frac{dU_{55c}^{39c}}{dt} = -(k_{21} + k_{32})U_{55c}^{39c} + k_{12}U_{55c}^{39t} + k_{23}U_{55t}^{39c} + k_{43}N \quad (1)$$

$$\frac{dU_{55c}^{39t}}{dt} = -(k_{32} + k_{12})U_{55c}^{39t} + k_{21}U_{55c}^{39c} + k_{23}U_{55t}^{39t} \quad (2)$$

$$\frac{dU_{55t}^{39t}}{dt} = -(k_{12} + k_{23})U_{55t}^{39t} + k_{32}U_{55c}^{39t} + k_{21}U_{55t}^{39c} \quad (3)$$

$$\frac{dN}{dt} = -k_{43}N \quad (4)$$

$$\Delta F = c_1(U_{55c}^{39c} + U_{55t}^{39c}) + c_2U_{55c}^{39t} \quad (5)$$

The $U_{55i}^{39i}$ and $N$ in eqs 1−5 represent the reduced concentrations of the individual species in Scheme 1. The sum of the reduced concentrations of all species is equal to 1. At the beginning of unfolding, the reduced concentrations of all unfolded species ($U_{55i}^{39i}$) are zero, and the reduced concentration of the native protein ($N$) is 1. The rate constant for refolding $k_{34}$ was set to zero, because strongly unfolding conditions were used in our experiments.

*Kinetics of Unfolding and Refolding of the S54G/P55N Variant.* The fast refolding of this variant was a single first-order reaction, which was assumed to reflect the direct folding reaction $U^{39c} \rightarrow N$ with a specific change in fluorescence of $c_1$ (eq 9).

The kinetics of unfolding and isomerization of the S54G/P55N variant are simplified because only a single *cis* ⇌ *trans* isomerization (of Pro39) is coupled with unfolding (Scheme 3).

Scheme 3: Mechanism of Unfolding and Isomerization of S54G/P55N-RNase T1

$$U^{39t} \underset{k_{21}}{\overset{k_{12}}{\rightleftharpoons}} U^{39c} \underset{k_{43}}{\overset{k_{34}}{\rightleftharpoons}} N$$

As for the wild-type protein, the dependence of the amplitudes of the direct refolding reaction on the duration of unfolding was used to determine the rate constants of unfolding ($k_{43}$) and of Pro39 isomerization ($k_{12}$ and $k_{21}$) in Scheme 3. The differential eqs 6−9 were employed. $c_1$ is the fit parameter for the specific fluorescence change during the direct folding reaction.

$$\frac{dU^{39c}}{dt} = -k_{21}U^{39c} + k_{12}U^{39t} + k_{43}N \quad (6)$$

$$\frac{dU^{39t}}{dt} = -k_{12}U^{39t} + k_{21}U^{39c} \quad (7)$$

$$\frac{dN}{dt} = -k_{43}N \quad (8)$$

$$\Delta F = c_1U^{39c} \quad (9)$$

The dependences on temperature of the fast refolding reactions were analyzed by using transition state theory and following the procedure employed by Chen *et al.* (1992).

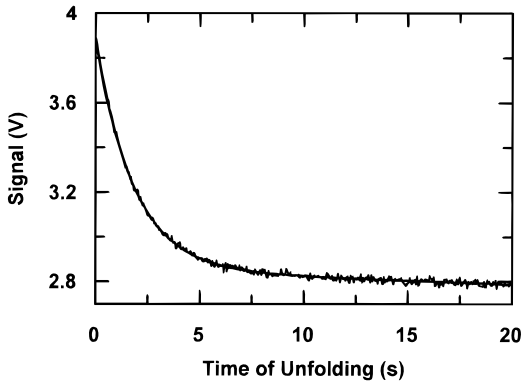


FIGURE 1: Stopped-flow unfolding kinetics of wild-type RNase T1 after a 6-fold dilution of native protein (6 $\mu$M in 0.01 M sodium acetate, pH 5.0) to final conditions of 0.083 M glycine hydrochloride, 6.0 M GdmCl (pH 1.6).Unfolding was measured by the decrease in protein fluorescence above 300 nm. The decrease in the photomultiplier voltage is shown as a function of the time of unfolding. The experimental curve was fit to the sum of a single-exponential function (with $\tau = 1.8$ s and $a = -1.03$ V) and a linear term with a slope of $m = -3.1 \times 10^{-3}$ V/s, as shown by the continuous line.

*Peptide Syntheses.* The tetrapeptide-4-nitroanilide derivatives Suc-Ser-Ser-Pro-Tyr-4-nitroanilide and Suc-Ser-Tyr-Pro-His-4-nitroanilide were synthesized by Fmoc-based solid phase synthesis, and the purity was examined by HPLC and by capillary electrophoresis. The structures were confirmed by $^1$H-NMR and by electrospray mass spectrometry.

*Kinetics of the cis/trans Isomerization in the Model Peptides.* The kinetics of *cis* → *trans* isomerization were determined by isomer-specific proteolysis by using subtilisin as the protease and the procedure devised by Fischer *et al.* (1984). In the experiments, $x$ $\mu$L of a 90 mg/mL solution of subtilisin in the assay buffer (0.083 M sodium acetate, pH 7.0) was mixed with (1200 − $x$) $\mu$L of the same buffer and preequilibrated in the spectrometer cell at the desired temperature. After 5 min, the reaction was initiated by adding 10 $\mu$L of a stock solution of the peptide derivative (3.2 mg/mL in the assay buffer), and the absorbance of the released 4-nitroaniline was followed at 390 nm ($\epsilon = 11\,814$ $M^{-1}$ $cm^{-1}$) in a Hewlett-Packard 8452A diode array spectrophotometer. The Hewlett-Packard 89531A MS-DOS UV/VIS operation software or SigmaPlot Scientific Graphing System Version 5.01 (Jandel Corp.) were used for data analysis. The final concentrations of subtilisin were 1.2 and 26.5 mg/mL for Suc-Ser-Ser-Pro-Tyr-4-nitroanilide and Suc-Ser-Tyr-Pro-His-4-nitroanilide, respectively. The analysis of the temperature dependence on the rate constant $k_{cis \rightarrow trans}$ was performed between 3.5 and 25 °C in triplicate experiments.

## RESULTS

*Unfolding Kinetics of RNase T1.* In a protein unfolding reaction, molecules with correct prolyl isomers ($U_{55c}^{39c}$) accumulate transiently at high concentration only when the N → $U_{55c}^{39c}$ unfolding reaction (Scheme 1) is much faster than the subsequent prolyl isomerizations. RNase T1 shows a high stability, and the N → $U_{55c}^{39c}$ unfolding reaction is slow under most conditions. Its rate could be increased, however, by raising the concentration of denaturant and by decreasing the pH. In 6.0 M GdmCl at pH 1.6 (25 °C), unfolding proceeded with a time constant of 1.8 s (Figure 1), which is

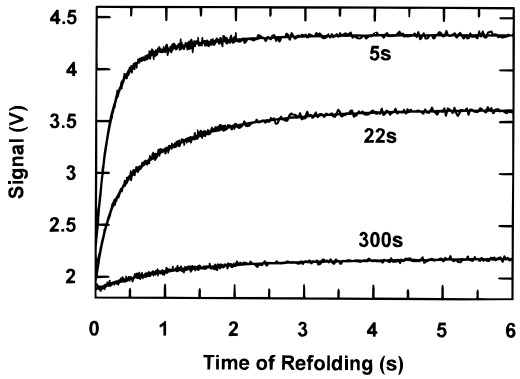


FIGURE 2: Refolding kinetics of wild-type RNase T1 after variable times of unfolding. In stopped-flow double-mixing experiments, unfolding was initiated by a 6-fold dilution of native protein (36 $\mu$M in 0.01 M sodium acetate, pH 5.0) to conditions of 0.083 M glycine hydrochloride, 6.0 M GdmCl (pH 1.6). Refolding was induced by a further 6-fold dilution to final folding conditions of 1 $\mu$M protein in 1.0 M GdmCl, 0.083 M sodium acetate, and 0.014 M glycine (pH 4.6). All experiments were carried out at 25 °C. The first 6 s of refolding is shown after 5 s (upper curve), 22 s (middle curve), and 300 s of unfolding (lower curve). Refolding was followed by the increase in protein fluorescence above 300 nm. The increase in the signal of the photomultiplier is shown as a function of the time of refolding. The experimental curves were fit to the sum of two exponential functions and a linear term with the slope *m*, which represents the onset of the slow refolding reaction. The fit parameters were as follows: (upper curve) $\tau_1 =$ 177 ms ($a_1 = 1.68$ V), $\tau_2 = 0.98$ s ($a_2 = 0.39$ V), $m = 2.7 \times 10^{-4}$ V/s; (middle curve) $\tau_1 = 168$ ms ($a_1 = 0.59$ V), $\tau_2 = 1.01$ s ($a_2 =$ 0.99 V), $m = 6.4 \times 10^{-3}$ V/s; (lower curve) $\tau_2 = 1.02$ s ($a_2 = 0.24$ V), $m = 9.1 \times 10^{-3}$ V/s. The fits are shown by the continuous lines.

about an order of magnitude faster than the subsequent isomerizations of Pro39 and Pro55 in the unfolded protein (see below). These strongly unfolding conditions were therefore used to produce the $U_{55c}^{39c}$ species in the first step of double-mixing experiments.

*Double-Mixing Experiments To Measure the Fast Refolding Reactions of RNase T1*. To measure the kinetics of refolding of the $U_{55c}^{39c}$ species, we used a double-mixing stopped-flow technique. In the first step, native RNase T1 was 6-fold-diluted to 6.0 M GdmCl, pH 1.6 (as in Figure 1), to unfold the protein, and then, after a short period of time, refolding was initiated in the second step by another 6-fold dilution to give a final concentration of 1.0 M GdmCl at pH 4.6. The time course of refolding after the second mixing was monitored by the increase in protein fluorescence above 300 nm. Representative kinetic traces obtained after 5, 22, and 300 s of unfolding are shown in Figure 2. They demonstrate that fast refolding species of RNase T1 are indeed present at high concentration after a short 5-s unfolding pulse, and that they refold rapidly. With increasing time of unfolding, both the amplitude and the final value of fast refolding decrease, and after 300 s of unfolding, fast refolding is barely detectable. The onset of the slow refolding reactions leads to a continuing increase in fluorescence after the completion of the fast changes in Figure 2. These slow reactions with time constants of 100 and 1000 s (Kiefhaber *et al.*, 1990a,b) could not be measured in the stopped-flow instrument because the fluorescence signal was not sufficiently stable for more than 3000 s. The observed fast refolding kinetics after 5 and 22 s of unfolding could not be fit to a single-exponential function. Rather, they consisted of two phases: refolding phase 1 with a time

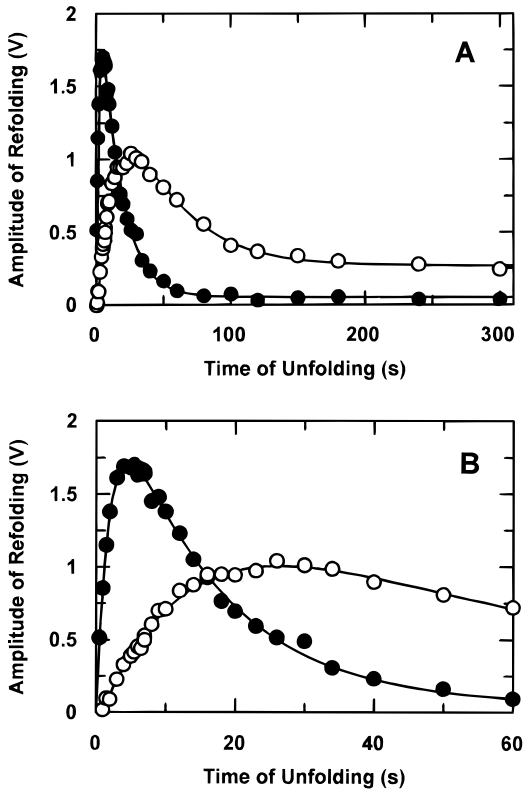


FIGURE 3: Amplitudes of phase 1 ($\tau_1 = 175 \pm 3$ ms) (●) and phase 2 ($\tau_2 = 1.01 \pm 0.02$ s) (○) of the the fast refolding of wild-type RNase T1 as a function of the duration of unfolding at 25 °C. The stopped-flow double-mixing experiments were carried out as in Figure 2. The data points reflect the amplitudes from single refolding experiments after the indicated times of unfolding. The entire time course of unfolding is shown in panel A; an expanded view of the first 60 s of unfolding is given in panel B. The lines represent a best fit of the data to the kinetic model in Scheme 1 by using eqs 1−5. The fit parameters are given in Table 1.

constant $\tau_1 = 175$ ms and refolding phase 2 with a time constant $\tau_2 = 1.01$ s.

*Fast Refolding after Variable Time Intervals of Unfolding.* Double-mixing experiments as in Figure 2 are not only useful to measure the refolding of transient species that are scarcely populated at equilibrium but they can also be used to identify the unfolded species which give rise to particular refolding reactions and to measure the kinetics of their formation and interconversion under unfolding conditions (cf. Scheme 1).

Therefore, in further double-mixing experiments (as in Figure 2), the duration of unfolding in the first step was varied from 0.5 to 300 s, and the rate constants and the amplitudes associated with the two fast refolding phases in the second step were determined as a function of the time of unfolding. Biphasic kinetics were observed in all cases. The time constants of both phase 1 ($\tau_1 = 175 \pm 3$ ms) and phase 2 ($\tau_2 = 1.01 \pm 0.02$ s) were independent of the duration of unfolding in the first step, but the corresponding amplitudes (Figure 3) depended strongly and in a different manner on the duration of unfolding. The amplitude of phase 1 ($a_1$) increased rapidly after the initiation of unfolding (Figure 3B), reached a maximal value of 1.7 V after about 5 s, and then decreased again, until a small limiting value of about 0.04 V was attained at unfolding times longer than 100 s (Figure 3A). The increase of the amplitude of phase 2 ($a_2$) was much slower. It paralleled the decrease of $a_1$, reached a maximum of 1.04 V after 25 s of unfolding, and then decreased slowly until a limiting value of about 0.25 V

Table 1: Microscopic Rate Constants of Unfolding and Isomerization of Wild-Type RNase T1 as a Function of Temperature[a]

| temp (°C) | $N \rightarrow U^{39c}_{55c}$, unfolding,[b] $k_{43}$ ($s^{-1}$) | Pro39 | | Pro55 | | $c_1$ (V) | $c_2$ (V) |
|---|---|---|---|---|---|---|---|
| | | *trans* → *cis*, $k_{12} \times 10^3$ ($s^{-1}$) | *cis* → *trans*, $k_{21} \times 10^3$ ($s^{-1}$) | *trans* → *cis*, $k_{23} \times 10^3$ ($s^{-1}$) | *cis* → *trans*, $k_{32} \times 10^3$ ($s^{-1}$) | | |
| 10 | 0.044 ± 0.003 | | 3.0 ± 0.2 | 3.7 ± 0.7 | 12.6 ± 0.8 | 2.27 ± 0.07 | 1.3 ± 0.3 |
| 15 | 0.100 ± 0.005 | 0.22 ± 0.21 | 6.3 ± 0.4 | 8.4 ± 1.1 | 22.5 ± 1.0 | 2.26 ± 0.05 | 0.94 ± 0.15 |
| 20 | 0.26 ± 0.01 | 1.0 ± 0.3 | 12.2 ± 0.4 | 5.4 ± 0.8 | 29.2 ± 1.4 | 2.60 ± 0.04 | 0.88 ± 0.29 |
| 25 | 0.49 ± 0.02 | 2.0 ± 0.4 | 22.6 ± 1.4 | 8.7 ± 3.3 | 50.5 ± 5.3 | 2.38 ± 0.03 | 0.81 ± 0.28 |
| 30 | 1.72 ± 0.05 | 3.8 ± 1.3 | 47.7 ± 2.7 | 20.9 ± 4.4 | 99.9 ± 6.1 | 2.63 ± 0.03 | 0.75 ± 0.32 |
| 35 | 4.84 ± 0.14 | 9.8 ± 1.9 | 86.6 ± 4.4 | 32.6 ± 5.7 | 185 ± 10 | 2.63 ± 0.03 | 0.71 ± 0.37 |
| 40 | 16 ± 1 | | 215 ± 20 | 111 ± 45 | 280 ± 30 | 2.30 ± 0.03 | 0.74 ± 0.19 |

[a] The kinetic parameters were derived from the analysis of double-mixing experiments as in Figures 2 and 5, by using Scheme 1 and eqs 1 −5. The microscopic rate constants refer to Scheme 1. $c_1$ is the specific change in fluorescence of the $U^{39c}_{55c} \rightarrow N$ and the $U^{39c}_{55t} \rightarrow I^{39c}_{55t}$ reaction; $c_2$ is the specific change in fluorescence of the $U^{39t}_{55c} \rightarrow I^{39t}_{55c}$ reaction. Values for $k_{12}$ are not given at 10 and 40 °C, because of the large uncertainties for these fit values. [b] The data refer to unfolding conditions of 6.0 M GdmCl in 0.83 M glycine hydrochloride, pH 1.6.

was reached at times longer than 300 s. The profiles for $a_1$ and $a_2$ in Figure 3 show that the species which refolds in phase 1 is formed by a process with a time constant of 2.1 s and decays with a time constant of 11 s. The molecules which refold in phase 2 are formed with a time constant of 17 s and decay with a time constant of 40 s. This analysis strongly suggests that the fastest phase indeed reflects the refolding of $U^{39c}_{55c}$, because the rate of its formation coincides with the rate of the $N \rightarrow U^{39c}_{55c}$ unfolding reaction (see Figure 1). $U^{39c}_{55c}$ is converted to species with incorrect prolyl isomers in the 17-s phase. The correlation between the decrease of $a_1$ and the increase of $a_2$, which is most clearly seen in Figure 3B, indicates that the species that give rise to refolding in phase 2 (with $\tau = 1.01$ s) are formed from the species that refolds in phase 1 (with $\tau = 175$ ms).

Refolding phase 1 persists with a very small amplitude even after long times of unfolding (Figure 3A). This reflects the small amount of $U^{39c}_{55c}$ molecules present at equilibrium (Schemes 1 and 2). Refolding phase 2 originates probably from one or more species that are formed from $U^{39c}_{55c}$ by prolyl isomerizations (in the 17-s phase), and it decays in the 40-s phase by reactions that also involve prolyl isomerizations. This suggests that one or both species with a single incorrect proline, $U^{39t}_{55c}$ and/or $U^{39c}_{55t}$, contribute to phase 2 ($\tau = 1.01$ s). The product of this folding reaction should thus be a folding intermediate with an incorrect proline (possibly $I^{39t}_{55c}$ and/or $I^{39c}_{55t}$ in Scheme 2). It is not the native protein. In refolding experiments after a very long time of unfolding, phase 2 contributes about 10−15% of the total amplitude (Figure 3A), but after its completion (about 10 s), only 2−4% of native RNase T1 molecules have formed, as determined earlier by assays for native molecules (Kiefhaber *et al.*, 1990b). These native molecules are formed only by the $U^{39c}_{55c} \rightarrow N$ reaction.

*Numerical Calculation of the Rate Constants of Unfolding and Isomerization.* The amplitude profiles in Figure 3 reflect the kinetics of unfolding ($N \rightarrow U^{39c}_{55c}$) and of the subsequent *cis* ⇌ *trans* isomerizations of Pro39 and Pro55 in the unfolded protein in Scheme 1. To determine the microscopic rate constants for these reactions, a nonlinear least-squares fit of the time dependences of the refolding amplitudes $a_1$ and $a_2$ (in Figure 3) to the kinetic model in Scheme 1 was performed by using the program EASY-FIT (Schittkowski, 1993). In this method, the differential rate equations for the individual species in Scheme 1 were used (eqs 1−4). The following assumptions were made in these calculations. (i) The rate constant of refolding, $k_{34}$, is virtually zero under the employed strongly unfolding conditions. (ii) The fastest phase of refolding (phase 1) reflects the refolding reaction $U^{39c}_{55c} \rightarrow N$. A significant contribution from the species with incorrect prolines to this reaction can be excluded, because its amplitude is almost zero after more than 100 s of unfolding (Figure 3A), when almost all unfolded molecules have incorrect prolyl isomers. The $U^{39c}_{55c} \rightarrow N$ reaction is accompanied by a change in fluorescence of magnitude $c_1$. (iii) Phase 2 in Figure 3 is assumed to originate from the refolding reactions $U^{39t}_{55c} \rightarrow I^{39c}_{55t}$ and $U^{39c}_{55t} \rightarrow I^{39c}_{55t}$ (cf. Scheme 2) of the unfolded species with a single incorrect proline. $I^{39c}_{55t}$ resembles N in its fluorescence (Kiefhaber *et al.*, 1990b, 1992a), and therefore a specific change in fluorescence of $c_1$ was assigned to the $U^{39c}_{55t} \rightarrow I^{39c}_{55t}$ reaction too. The change in fluorescence in the $U^{39t}_{55c} \rightarrow I^{39t}_{55c}$ reaction was not known and is represented by the fit parameter $c_2$ in eq 5. (iv) $I^{39t}_{55t}$ is similar to $U^{39t}_{55t}$ in its fluorescence, and therefore the $U^{39t}_{55t} \rightarrow I^{39t}_{55t}$ reaction does not contribute to the refolding phase 2. $U^{39t}_{55t}$ is the dominant species after more than 100 s of unfolding, and the small amplitude of phase 2 after 300 s of unfolding (Figure 3) excludes a significant contribution of $U^{39t}_{55t} \rightarrow I^{39t}_{55t}$ to the refolding phase 2.

The parameters resulting from the fit of the amplitudes of refolding in Figure 3 to the model in Scheme 1 are included in Table 1. The rates of *cis* → *trans* isomerization of the two prolines in the unfolded protein are not identical, but differ by about a factor of 2. At this stage of the work, we could not assign these two isomerizations specifically to Pro39 and Pro55, because the kinetic model in Scheme 1 is inherently symmetric. The assignment was possible, however, by including the kinetic data for the variants with substitutions at Pro39 (Odefey *et al.*, 1995) and Pro55 (see below). The kinetic results in Table 1 will therefore be discussed later together with the results obtained for these variants. The values for the microscopic rate constants and for $c_1$ and $c_2$ at 25 °C (Table 1) describe the dependence of the amplitudes $a_1$ and $a_2$ on the duration of unfolding very well (cf. the continuous lines in Figure 3).

The microscopic rate constants obtained at 25 °C were used to calculate the concentrations of the native and the various unfolded species as a function of the time of unfolding (Figure 4). The concentration of the native protein N decreases rapidly at the beginning in the $N \rightarrow U^{39c}_{55c}$ unfolding reaction. This reaction is virtually complete after

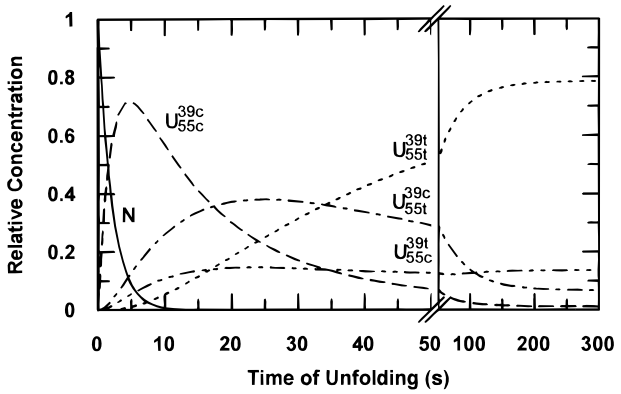


FIGURE 4: Time courses of the various folded and unfolded forms of wild-type RNase T1 during unfolding in 0.083 M glycine hydrochloride, 6.0 M GdmCl (pH 1.6) at 25 °C. The profiles for the individual species were calculated by using the rate constants for 25 °C given in Table 1. (—) N; (— —) $U_{55c}^{39c}$; (— - - —) $U_{55c}^{39t}$; (— - —) $U_{55t}^{39c}$; (- - -) $U_{55t}^{39t}$.

about 10 s, and most molecules are in the $U_{55c}^{39c}$ state with both Pro39 and Pro55 still in the native *cis* conformation at this time. The profile for $U_{55c}^{39c}$ follows the profile for $a_1$ in Figure 3. Then the two *cis* → *trans* isomerizations occur, and 20 s after the initiation of unfolding, the species $U_{55c}^{39t}$ and $U_{55t}^{39c}$ with a single incorrect *trans* prolyl isomer each are strongly populated. The species with two *trans* isomers, $U_{55t}^{39t}$, is formed most slowly with a lag at the beginning, because it is formed from $U_{55c}^{39c}$ via $U_{55c}^{39t}$ or $U_{55t}^{39c}$ in sequential reactions (cf. Scheme 1). At equilibrium (after about 300 s), about 78% $U_{55t}^{39t}$ is present, together with 13% $U_{55c}^{39t}$, 8% $U_{55t}^{39c}$, and 3% $U_{55c}^{39c}$.

The concentration profiles in Figure 4 emphasize the power of the double-mixing technique. Although the fast folding species $U_{55c}^{39c}$ is barely populated when RNase T1 is unfolded at equilibrium, an unfolding pulse of 5 s made it possible to produce this species transiently at a very high concentration and to study the kinetics of its refolding.

*Dependence on Temperature of the Rates of Unfolding and Isomerization.* Series of double-mixing experiments as in Figure 3 were performed at seven different temperatures between 10 and 40 °C. The results obtained at 10 and at 35 °C are shown in Figure 5A,B. At all temperatures, the two phases of refolding in the second step could be resolved, and the measured rate constants of refolding were independent of the duration of unfolding in the first step. As at 25 °C (Figure 3), the amplitudes $a_1$ and $a_2$ of the two phases of refolding showed strongly different dependences on the time of unfolding in the first step. They were analyzed as outlined for the data at 25 °C (in Figure 3) by using Scheme 1 and eqs 1−5. The resulting values for all microscopic rate constants and for $c_1$ and $c_2$ are listed in Table 1 as a function of temperature. The fit to the experimental data was generally good at temperatures higher than 15 °C (cf. Figure 3 and Figure 5B). At 10 and 15 °C, small systematic deviations between the experimental data and the calculated curves were found (cf. Figure 5A). It is possible that some of the assumptions that were made in the kinetic analysis do not hold at low temperature. In particular, the species with two incorrect isomers ($U_{55t}^{39t}$) might contribute to phase 2 of refolding. The dependences on temperature of the two rate constants for *cis* → *trans* isomerization, $k_{21}$ and $k_{32}$, are

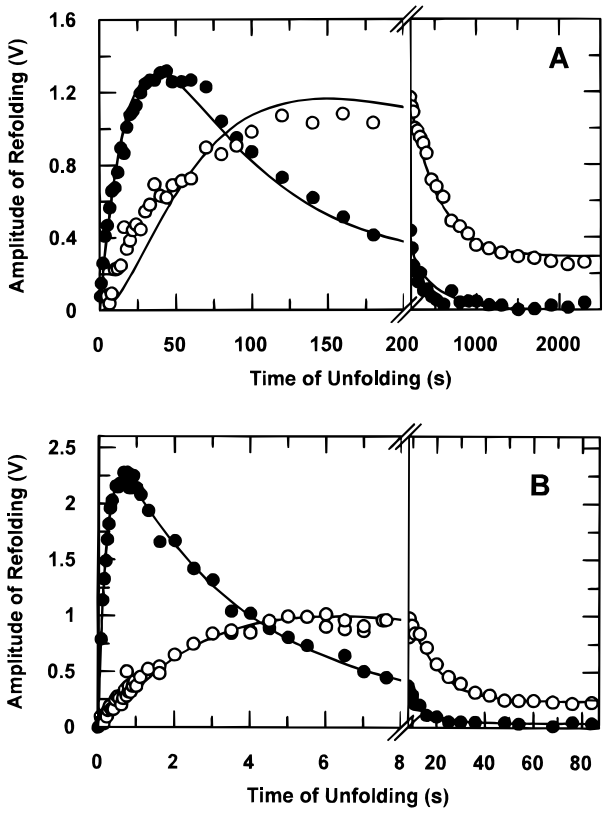


FIGURE 5: Kinetics of unfolding and isomerization of wild-type RNase T1 at (A) 10 °C and (B) 35 °C. As in Figure 3, the amplitudes of phase 1 (●) and phase 2 (○) of fast refolding are shown as a function of the duration of unfolding. The stopped-flow double-mixing experiments were carried out as described in Figures 2 and 3. The lines represent best fits of the data to the kinetic model in Scheme 1 by using eqs 1−5. The fit parameters are given in Table 1.

shown in Figure 11 together with the isomerization rate constants of the proline mutants (see below).

*Dependence on Temperature of the Rates of Refolding.* The double-mixing experiments at the various temperatures also gave information on the temperature dependence of the two fast refolding reactions, $U_{55c}^{39c}$ → N (phase 1) and ($U_{55c}^{39t}$ + $U_{55t}^{39c}$) → ($I_{55c}^{39t}$ + $I_{39c}^{55t}$) (phase 2). The apparent rate constants of these two folding reactions ($\tau_1^{-1}$ and $\tau_2^{-1}$) are plotted as a function of temperature in Figure 6. Both show similar complex dependences on temperature with maximal rates near 25 °C. All the experiments of Figure 6 are carried out in the native base-line region of thermal unfolding, and therefore $\tau_1^{-1}$ should be identical to the microscopic rate constant of refolding $k_{34}$. Less is known about the thermal stability of the intermediates with incorrect prolines, which are formed in phase 2. A tentative analysis of the data in Figure 6 based on transition state theory results in values of 69 and 73 kJ/mol for the Gibbs free energy of activation (at 25 °C) for phase 1 and phase 2, respectively. The pronounced nonlinearity points to changes in the heat capacity of activation of −3.3 kJ/(K·mol) for phase 1 and of −2.8 kJ/(K·mol) for phase 2.

The strong deviation of the rate of phase 2 ($\tau_2^{-1}$) between 40 and 42 °C from the curve in Figure 6 indicates that $\tau_2^{-1}$ can no longer be equated with the microscopic rate constant of refolding of the intermediates with incorrect prolines. These intermediates are probably less stable than native RNase T1 and enter their unfolding transition already near

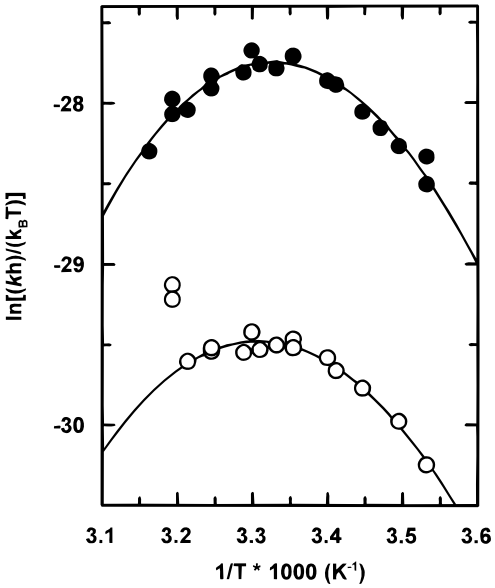


FIGURE 6: Eyring plots of the dependence on temperature of the measured rate constants of (●) phase 1 and (○) phase 2 of the fast refolding kinetics of wild-type RNase T1. The refolding conditions were 1.0 M GdmCl in 0.083 M sodium acetate, 0.014 M glycine (pH 4.6). The data points represent average rate constants from at least 10 individual refolding experiments. The continuous lines represent fits (Chen *et al.*, 1989) to the data resulting in values of $\Delta G^{\ddagger} = 69$ kJ/mol (at 25 °C) and $\Delta C_p^{\ddagger} = -3.2$ kJ/(K·mol) for phase 1 and of $\Delta G^{\ddagger} = 73$ kJ/mol (at 25 °C) and $\Delta C_p^{\ddagger} = -2.8$ kJ/(K·mol) for phase 2. For phase 2, the two points at $1/T = 0.00318$ $K^{-1}$ were not included into the fit.

40 °C. This is supported by the finding that the amplitude of this reaction ($a_2$) approaches zero above 42 °C.

*Unfolding Kinetics of S54G/P55N-RNase T1.* S54G/P55N-RNase T1 contains only a single *cis* proline (Pro39), and the kinetics of its refolding are strongly simplified (Kiefhaber *et al.*, 1990c). We investigated the unfolding and refolding kinetics of this variant also by the stopped-flow double-mixing technique (i) to identify the isomerization of Pro39 in the unfolded wild-type protein from a comparison of S54G/P55N-RNase T1 and the wild-type protein and (ii) to characterize the influence of the substitutions of Ser54 and *cis* Pro55 on the direct folding reaction, which does not involve prolyl isomerizations. In the $U^{39c}_{55c} \rightarrow N$ reaction of wild-type RNase T1, the protein folds with a *cis* Ser54−Pro55 bond, but in the $U^{39c} \rightarrow N$ reaction of the S54G/P55N variant, the protein folds with a *trans* Gly54−Asn55 bond.

Unfolding of S54G/P55N-RNase T1 in the presence of 6.0 M GdmCl, pH 1.6 (Figure 7), is also a single first-order reaction. With its time constant of 610 ms, it is about 3-fold faster than the unfolding of the wild-type protein under the same conditions (cf. Figure 1). Representative kinetics of fast refolding after various times of unfolding are shown in Figure 8. After 0.1 s of unfolding, most of the protein is still native. Only a very small rapid refolding reaction is monitored after the second mixing, and the fluorescence of the native protein is regained within about 1 s. With increasing duration of unfolding in the first step, more $U^{39c}$ molecules (with a native-like *cis* Pro39) are produced. Therefore, the initial fluorescence before refolding in the second step decreases, and the amplitude of the rapid refolding reaction increases. After 5 s, the protein is completely unfolded, but almost all molecules are still in the $U^{39c}$ state and refold rapidly in a single first-order reaction

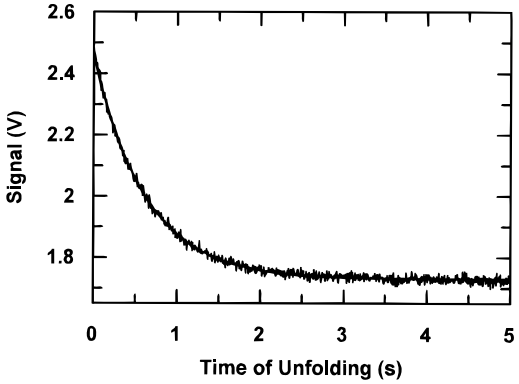


FIGURE 7: Kinetics of unfolding of S54G/P55N-RNase T1 after a 6-fold dilution of native protein (6 $\mu$M in 0.01 M sodium acetate, pH 5.0) to 0.083 M glycine hydrochloride, 6.0 M GdmCl (pH 1.6). Unfolding was measured as described in Figure 1. The experimental data were fit to a single-exponential function with $\tau = 610$ ms and $a = -0.72$ V. The fit is shown by the continuous line.

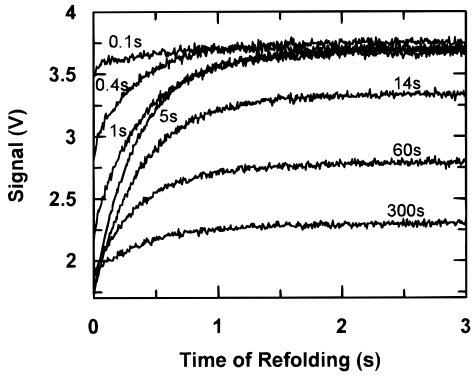


FIGURE 8: Refolding kinetics of S54G/P55N-RNase T1 after variable times of unfolding. In stopped-flow double-mixing experiments, unfolding was initiated by a 6-fold dilution of native protein (36 $\mu$M in 0.01 M sodium acetate, pH 5.0) to conditions of 0.083 M glycine hydrochloride, 6.0 M GdmCl (pH 1.6). Refolding was induced by a subsequent 6-fold dilution to final folding conditions of 1 $\mu$M protein in 1.0 M GdmCl, 0.083 M sodium acetate, 0.014 M glycine (pH 4.6). All experiments were carried out at 25 °C. The first 3 s of refolding is shown after 0.1−300 s of unfolding (see labeling of the individual traces). Refolding was followed by the increase in protein fluorescence above 300 nm.

with a time constant of 380 ms (and an amplitude of 2.2 V). When the duration of unfolding is further increased, the amplitude of this fast refolding reaction decreases again, until a limiting value of about 0.35 V is reached after 300 s of unfolding. The fast reaction is followed by a steady increase in fluorescence. It reflects the onset of the slow refolding of the $U^{39t}$ molecules ($\tau = 800$ s; Kiefhaber & Schmid, 1992). A fast formation of an intermediate with an incorrect *trans* Pro39 could not be detected by fluorescence.

The amplitude of the fast refolding reaction of S54G/P55N-RNase T1 is shown in Figure 9 as a function of the time of unfolding. The corresponding time constant of refolding ($\tau = 400 \pm 10$ ms) was independent of the duration of unfolding. The amplitude reached a maximal value of 2.3 V after about 3 s, and then it decreased slowly until a limiting value of about 0.38 V was reached after about 200 s. Only a single *cis* proline (Pro39) is present in S54G/P55N-RNase T1, and the three-species mechanism in Scheme 3 and eqs 6−9 could be used to determine the rate constants of unfolding and of Pro39 isomerization from the refolding data in Figure 3. This analysis yielded a time constant of 620 ± 20 ms for the $N \rightarrow U^{39c}$ unfolding reaction, and time

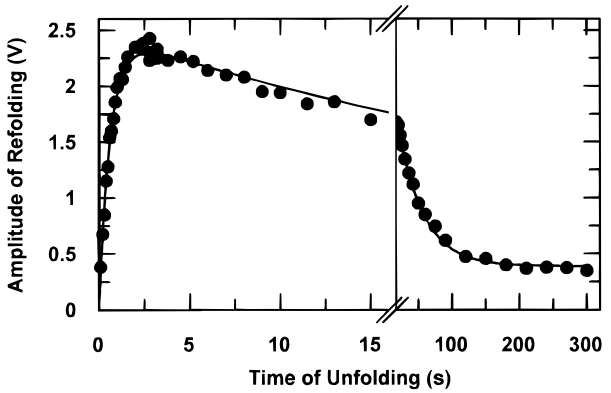


FIGURE 9: Amplitude of the fast refolding reaction of S54G/P55N-RNase T1 ($\tau$ = 377 ± 3 ms) as a function of the duration of unfolding at 25 °C. The stopped-flow double-mixing experiments were carried out as in Figure 8. The line represents a best fit of the data to the kinetic model in Scheme 3 by using eqs 6−9. The fit parameters are given in Table 2.

Table 2: Microscopic Rate Constants of Unfolding and Pro39 Isomerization of S54G/P55N RNase T1 as a Function of Temperature[a]

| temp (°C) | $N \rightarrow U^{39c}_{55c}$, unfolding,[b] $k_{43}$ ($s^{-1}$) | Pro39, *trans* → *cis*, $k_{12} \times 10^3$ ($s^{-1}$) | Pro39, *cis* → *trans*, $k_{21} \times 10^3$ ($s^{-1}$) | $c_1$ (V) |
|---|---|---|---|---|
| 10 | 0.172 ± 0.005 | 0.38 ± 0.05 | 3.0 ± 0.1 | 2.42 ± 0.02 |
| 15 | 0.35 ± 0.01 | 0.95 ± 0.08 | 6.00 ± 0.17 | 2.32 ± 0.02 |
| 20 | 0.74 ± 0.02 | 2.3 ± 0.5 | 11.7 ± 1.0 | 2.24 ± 0.05 |
| 25 | 1.62 ± 0.04 | 4.1 ± 1.0 | 21.9 ± 2.0 | 2.44 ± 0.05 |
| 30 | 3.96 ± 0.11 | 7.9 ± 0.7 | 37.7 ± 1.3 | 2.19 ± 0.02 |
| 35 | 9.8 ± 0.4 | 10.4 ± 1.1 | 67.4 ± 2.9 | 2.21 ± 0.02 |
| 40 | 26.8 ± 0.4 | 16.6 ± 2.4 | 126 ± 5.6 | 2.05 ± 0.02 |

[a] The kinetic parameters were derived from the analysis of double-mixing experiments as in Figure 9, by using Scheme 3 and eqs 6−9. The microscopic rate constants refer to Scheme 3. $c_1$ is the specific change in fluorescence of the $U^{39c}_{55c} \rightarrow N$ reaction. [b] The data refer to unfolding conditions of 6.0 M GdmCl in 0.83 M glycine hydrochloride, pH 1.6.

constants of 46 s for the *cis* → *trans* and 242 s for the *trans* → *cis* isomerizations of Pro39 in the unfolded protein. This suggests that an equilibrium mixture of 16% *cis* and 84% *trans* isomers is attained for Pro39 in unfolded S54G/P55N-RNase T1, in agreement with the values estimated previously (Kiefhaber *et al.*, 1990a,b; Kiefhaber & Schmid, 1992) by different methods.

*Dependence on Temperature of the Rates of Unfolding and Isomerization of S54G/P55N-RNase T1.* For S54G/P55N-RNase T1, the rates of refolding, unfolding, and Pro39 isomerization were also determined from double-mixing experiments as in Figure 9 between 10 and 40 °C. At all temperatures, refolding in the second step was a monophasic reaction, and the measured rate constant of refolding did not depend on the duration of unfolding in the first step. All results were analyzed as outlined for the data at 25 °C (in Figure 9) by using Scheme 3 and eqs 6−9. The microscopic rate constants for unfolding and for the isomerization of Pro39 obtained from these fits are given in Table 2 as a function of temperature. The time courses of the amplitude of fast refolding calculated with the parameters in Table 2 agreed very well with the experimental data at all temperatures.

The dependence on temperature of the rate constant of the direct refolding reaction, $U^{39c} \rightarrow N$, for S54G/P55N-RNase T1 is shown in Figure 10. As in the case of the wild-type protein (Figure 6), a pronounced nonlinearity is observed in the Eyring plot. The rate of direct refolding increases with temperature, reaches a maximum near 30 °C, and then decreases again. A tentative analysis based on transition state theory results in a value of 71 kJ/mol for the Gibbs free energy of activation (at 25 °C) and of −2.3 kJ/(K·mol) for the change in heat capacity of activation.

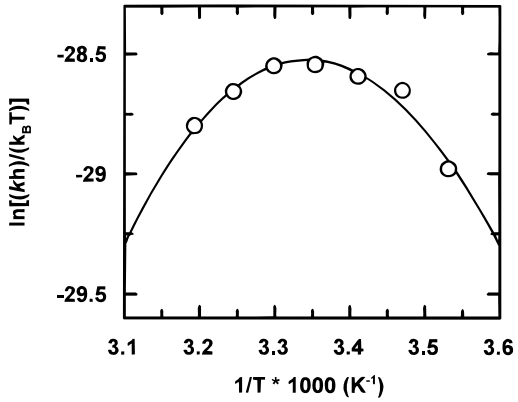


FIGURE 10: Eyring plot of the dependence on temperature of the rate constant of the direct (fast) refolding reaction of S54G/P55N-RNase T1. The refolding conditions were 1.0 M GdmCl in 0.083 M sodium acetate, 0.014 M glycine (pH 4.6). The continuous line represents a fit to the data resulting in $\Delta G^{\ddagger} = 71$ kJ/mol (at 25 °C) and $\Delta C_p^{\ddagger} = -2.3$ kJ/(K·mol).

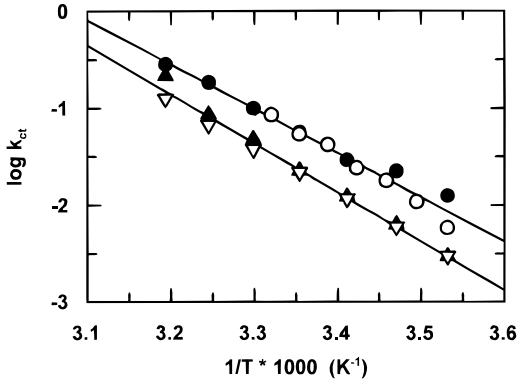


FIGURE 11: Dependence on temperature of the rate constants of Pro39 and of Pro55 *cis* → *trans* isomerization in unfolded RNase T1 in 6.0 M GdmCl (pH 1.6). Rate constant $k_{21}$ for the *cis* → *trans* isomerization of Pro39 in (▲) the wild-type protein and (▽) the S54G/P55N variant. Rate constant $k_{32}$ for the *cis* → *trans* isomerization of Pro55 in (●) the wild-type protein and (○) the P39A variant. The data for the P39A variant are taken from Odefey et al. (1995). The lines yield Arrhenius activation energies of 97 ± 3 kJ/mol for Pro39 and 87 ± 5 kJ/mol for Pro55. The rate constants for the *cis* → *trans* isomerizations were determined from the analysis of stopped-flow double-mixing experiments as in Figures 3, 5, and 9 at varying temperature as given in Tables 1 and 2 and by Odefey et al. (1995).

*Identification of the Isomerizations of Pro39 and Pro55 in Unfolded Wild-Type RNase T1.* The wild-type protein contains two *cis* prolines (Pro39 and Pro55), and two isomerizations were detected in the unfolded protein by the kinetic analysis (as compiled in Table 1). Their rate constants $k_{21}$ and $k_{32}$ are shown in Figure 11 as a function of temperature. The slower isomerization with the rate constant $k_{21}$ could be assigned to Pro39, because it coincides with the isomerization in the S54G/P55N variant (which contains only Pro39), and the faster isomerization with the rate constant $k_{32}$ could be assigned to Pro55, because it

Table 3: Microscopic Rate Constants for Prolyl *cis* → *trans* Isomerization in Model Peptides[a]

| temp (°C) | -Tyr-Pro-His-, $k_{cis\rightarrow trans}$ × $10^3$ ($s^{-1}$) | -Ser-Pro-Tyr-, $k_{cis\rightarrow trans}$ × $10^3$ ($s^{-1}$) |
|---|---|---|
| 3.3 | 2.45 | 4.61 |
| 8.6 | 5.22 | 7.93 |
| 11.7 | 7.84 | 11.1 |
| 16.0 | 11.2 | 16.1 |
| 17.5 | 14.0 | 21.0 |
| 20.5 | 19.4 | 27.8 |
| 25.0 | 30.0 | nd |

[a] The rate constants of *cis* → *trans* isomerization, $k_{cis\rightarrow trans}$, were measured by isomer-specific proteolysis as described under Materials and Methods. The isomerizations of -Tyr-Pro-His- and -Ser-Pro-Tyr- were followed in Suc-Ser-Tyr-Pro-His-4-nitroanilide and in Suc-Ser-Tyr-Pro-His-4-nitroanilide, respectively.

coincides with the previously measured isomerization in the P39A variant, which contains only Pro55 (Odefey *et al.*, 1995).

Since the rates for the *trans* → *cis* isomerizations have been determined as well (Tables 1 and 2), the equilibrium constants $K_{eq}$ = [*trans*]/[*cis*] could be calculated from the kinetic data. They are not very precise, because the accuracy of the rate constants for the *trans* → *cis* isomerizations from the joint fits is fairly low. They suggest, however, that in the unfolded protein about 15% of Pro39 and 15−20% of Pro55 are in the native-like *cis* conformation. The Arrhenius activation energies for *cis* → *trans* isomerization are 97 ± 3 and 88 ± 4 kJ/mol for Pro39 and Pro55, respectively.

*Isomerization of Prolines in Model Peptides.* To find out whether the rates of prolyl isomerization in unfolded RNase T1 are determined by the local amino acid sequence, we synthesized the two oligopeptides Suc-Ser-Tyr-Pro-His-4-nitroanilide and Suc-Ser-Ser-Pro-Tyr-4-nitroanilide. These peptides encompass the local sequences Ser37−His40 around Pro39 and Ser53−Tyr56 around Pro55, respectively, of RNase T1, and they can be cleaved by subtilisin in an isomer-specific manner when the Xaa−Pro bond is *trans*. The *cis*/*trans* equilibria and the rates of *cis* → *trans* isomerization were measured for these peptides between 3 and 25 °C by the protease-coupled assay devised by Fischer *et al.* (1984).

At 20.5 °C, a value of 19.4 × $10^{-3}$ $s^{-1}$ was found for $k_{cis\rightarrow trans}$ in the peptide Suc-Ser-Tyr-Pro-His-4-nitroanilide and a value of 27.8 × $10^{-3}$ $s^{-1}$ for Suc-Ser-Ser-Pro-Tyr-4-nitroanilide (Table 3). As in unfolded RNase T1, in the peptides the isomerization of -Tyr-Pro is slower than the isomerization of Ser-Pro. At 20 °C, the rate constants for the latter isomerization are identical in the peptide and in the unfolded protein (cf. Tables 1 and 3). For Ser-Tyr-Pro-His, the isomerization is slightly slower in the unfolded protein ($k_{cis\rightarrow trans}$ = 12.2 × $10^{-3}$ $s^{-1}$) than in the peptide ($k_{cis\rightarrow trans}$ = 19.4 × $10^{-3}$ $s^{-1}$). For Suc-Ser-Ser-Pro-Tyr-4-nitroanilide, 13% of the peptide was found to be in the *cis* conformation, in good agreement with the value estimated for Pro55 in unfolded RNase T1. For Suc-Ser-Tyr-Pro-His-4-nitroanilide, the *cis* content was 27%, which is somewhat higher than the value of 15% estimated for Pro39 in the unfolded protein. It is possible that in the peptide the 4-nitroanilide and the tyrosine residue prior to the proline are engaged in weak hydrophobic interactions that slightly favor the *cis* conformation.

The Arrhenius activation energies for *cis* → *trans* isomerization were 70.8 kJ/mol for Suc-Ser-Ser-Pro-Tyr-4-nitroanilide and 78.5 kJ/mol for Suc-Ser-Tyr-Pro-His-4-nitroanilide. The rank order of these activation energies is the same as for the respective positions in unfolded RNase T1. In the peptides, both values are, however, about 18 kJ/mol smaller than in the unfolded protein. At present, we cannot offer a simple explanation for this difference.

## DISCUSSION

*Contributions of the cis Prolines 39 and 55 to the Folding Mechanism of RNase T1.* The roles of the two *cis* prolines for the mechanism of unfolding of RNase T1 could be dissected in the present study. The stopped-flow double-mixing experiments with the wild-type protein (with both *cis* prolines), the S54G/P55N variant (with *cis*-Pro39 only, this work), and the P39A variant [with *cis*-Pro55 only (Odefey *et al.*, 1995)] enabled us to identify these isomerizations in the unfolded wild-type protein and to measure their kinetics individually. The data obtained for the wild-type and for the variant proteins strongly support the kinetic mechanism for the unfolding and the isomerizations of RNase T1 that was proposed in Scheme 1. Small deviations were found only at 10 and 15 °C, probably because some simplifying assumptions that were made in the analysis of the refolding kinetics are not strictly met at low temperature.

The individual isomerizations of Pro39 and Pro55 could be identified, because they occurred with identical rates in the wild-type protein and in variants which contained single *cis* prolines only. The *cis* ⇌ *trans* isomerization of Ser54-Pro55 is about 2-fold faster than the isomerization of Tyr38-Pro39. Apparently, this difference reflects the local influence of the residues before and after the proline on the rate of isomerization. Strongly similar isomerization rates and *cis*/*trans* equilibria were found for Ser54-Pro55 and Tyr38-Pro39 either in the unfolded protein or in two oligopeptides that contained these prolyl bonds in the same local sequence as in RNase T1. This confirms that nonlocal interactions are absent around these prolines in unfolded RNase T1, and therefore the kinetics of their *cis*/*trans* isomerizations are determined only by the local amino acid sequence.

The Arrhenius activation energies (97 ± 3 and 88 ± 5 kJ/mol for Pro39 and Pro55 isomerization in unfolded RNase T1 and 78.5 and 70.8 kJ/mol for the respective isomerizations in the peptides) show the same rank order, but the absolute values are higher in the protein. They are, however, in the range expected from the data on other short peptides (Cheng & Bovey, 1977; Grathwohl & Wüthrich, 1981; Stein, 1993; Eberhardt *et al.*, 1993). The *cis*/*trans* equilibria at the two prolines are similar, and we estimate that Pro39 and Pro55 are 12−17% and 15−20%, respectively, in the *cis* conformation in the unfolded protein. These estimates are not very precise, because the rate constants for the minor *trans* → *cis* isomerizations ($k_{12}$ and $k_{23}$) could not be determined with high accuracy. They are the slowest processes in Scheme 1 and are therefore strongly sensitive to variations in the final fluorescence values reached in the refolding kinetics. In our previous analyses of the folding kinetics of RNase T1, we had not been able to resolve the isomerizations of Pro39 and Pro55 individually and had tentatively assumed that Pro39 and Pro55 isomerize with the same rates in unfolded RNase T1 (Kiefhaber *et al.*, 1990b; Mücke & Schmid, 1994b).

It should be noted that the two *trans* prolines (Pro60 and Pro73) are not accounted for in Scheme 1. In the unfolded state, only a minor fraction of all molecules contains incorrect *cis* isomers of these prolines, and therefore their contributions to the measured kinetics of refolding should be very small. Indeed, the substitution of one of them, Pro73, does not measurably affect the folding kinetics (T. Schindler et al., unpublished results).

*Direct Refolding Reactions of RNase T1.* The direct refolding reaction of the $U_{55c}^{39c}$ molecules with correct *cis* isomers at Pro39 and Pro55 could not be measured earlier, because only 2−4% of those molecules exist at equilibrium in the unfolded state. By the stopped-flow double-mixing procedure, we could now increase the concentration of $U_{55c}^{39c}$ transiently and determine the time constant of its refolding as 180 ms. $U_{55c}^{39c}$ is the first unfolded species and is formed directly from N. The amplitude of its refolding reaction increased with the same kinetics as the native molecules disappeared, and it decreased with a rate equivalent to the sum of the rates of Pro39 and Pro55 isomerization. This is expected, because either isomerization converts $U_{55c}^{39c}$ into slow folding molecules. This amplitude profile distinguishes the direct refolding reaction ($\tau = 180$ ms) from the 1.01-s refolding reaction. The molecules that give rise to the latter reaction are formed slowly by prolyl isomerization and decay slowly by prolyl isomerizations; i.e., this is a refolding reaction that originates from molecules with incorrect prolyl isomers (see below).

The measured rate constant of the direct refolding reaction shows a pronounced nonlinear dependence on temperature in an Eyring plot (Figure 6) with a maximum near 25 °C. This curvature is well accounted for by a change in the heat capacity of activation, $C_p^{\ddagger} = -3.3$ kJ/(K·mol). This value is equivalent to about two-thirds of the equilibrium change $\Delta C_p = -5.2$ kJ/(K·mol) upon folding (Kiefhaber *et al.*, 1990d; Hu *et al.*, 1992; Yu *et al.*, 1994), suggesting that the activated state shows a significant amount of native-like structure. A nonlinear dependence on temperature of the rates was observed previously in the refolding of several proteins and also interpreted with respect to the properties of the transition state (Hagerman & Baldwin, 1976; Pohl, 1976; Segawa & Sugihara, 1984; Chen *et al.*, 1992; Oliveberg *et al.*, 1995). Since both polar and nonpolar interactions contribute to the changes in heat capacity (Privalov & Makhatadze, 1992), a further interpretation of the value of $\Delta C_p^{\ddagger}$ is not warranted. The extent of hydrophobic interactions in the elusive activated state or the ensemble of activated states cannot be inferred easily from $\Delta C_p^{\ddagger}$.

The replacements of the *cis* prolines have only very small effects on the time constant of the direct folding reaction. It increases slightly to 300 ms for the P39A variant (Odefey *et al.*, 1995) and to 380 ms for the S54G/P55N variant (this study). For the latter species, this is not surprising, since the S54G/P55N double mutation is only weakly destabilizing. It is surprising, however, for the P39A variant, because the conformational stability of RNase T1 is reduced by about 21 kJ/mol by the P39A mutation (Mayr *et al.*, 1993b). This strong destabilization apparently does not originate from a decreased folding rate of the molecules that still retained the Tyr38−Ala39 bond in the native-like *cis* conformation. It appears that about 11 kJ/mol of the destabilization is explained by the 100-fold increase in the rate of unfolding and that, by difference, the strained *cis* Tyr38−Ala39 bond should destabilize the P39A variant by about 10 kJ/mol. Such a value would be expected for a *cis*/*trans* ratio of 1/100 at this bond in the unfolded protein, in agreement with theoretical estimates for the *cis*/*trans* equilibrium at peptide bonds (Ramachandran & Mitra, 1976; Jorgensen & Gao, 1988).

*Formation of Transient Intermediates with an Incorrect Proline.* The rapid double-mixing experiments revealed a second fast phase in the refolding of RNase T1 with a time constant of 1.01 s at 25 °C. The amplitude profile for this phase strongly suggests that both the formation and the decay of the species that give rise to this phase involve prolyl isomerizations. We propose that the two unfolded species with a single incorrect isomer, $U_{55c}^{39t}$ and $U_{55t}^{39c}$ (cf. Scheme 2), are involved and that the 1.01-s phase reflects the formation of the partially folded intermediates $I_{55c}^{39t}$ and $I_{55t}^{39c}$ (Scheme 2). It can be excluded that the $U_{55t}^{39t}$ species with two incorrect isomers contributes significantly to the 1.01-s phase, because its amplitude becomes very small after extended times of unfolding, when $U_{55t}^{39t}$ is strongly populated.

Surprisingly, the folding reaction of the species with an incorrect proline isomer (to intermediates which still have an incorrect proline isomer) is only about 5-fold slower than the direct folding reaction of $U_{55c}^{39c}$ to the native state. Furthermore, it strongly resembles direct folding in its nonlinear dependence on temperature in the Eyring plot (Figure 6) and, consequently, in $\Delta C_p^{\ddagger}$. This may indicate that the activated states for the folding in the presence and in the absence of incorrect prolyl isomers bear some resemblance. In contrast to these similarities in refolding, the native protein and the folding intermediates with incorrect prolines differ strongly in the rate of unfolding (Kiefhaber *et al.*, 1990b). It should be noted that in the refolding of the constant domain of the immunoglobulin light chain the direct folding reaction and the formation of intermediates with incorrect prolines also coincided kinetically (Goto & Hamaguchi, 1982).

In the past, it has not been possible to characterize the contributions of individual prolines to the folding mechanism of a protein. The combination of proline mutagenesis, stopped-flow double-mixing experiments, and peptide synthesis has advanced our knowledge significantly. It enabled us to characterize the contributions of Pro39 and Pro55 to the folding of RNase T1, and, in addition, it led to the detection and the characterization of a non-prolyl peptide bond isomerization in the folding of the P39A variant of this protein.

## ACKNOWLEDGMENT

We thank Klaus Schittkowski for making his program EASY-FIT available to us and Vishwas Agashe, Gunter, Fischer, Thomas Schindler, Volker Sieber, and Stefan Walter for discussions of this work.

## REFERENCES

Bächinger, H.-P. (1987) *J. Biol. Chem. 262*, 17144−17148.

Brandts, J. F., Halvorson, H. R., & Brennan, M. (1975) *Biochemistry 14*, 4953−4963.

Chen, B. L., Baase, W. A., Nicholson, H., & Schellman, J. A. (1992) *Biochemistry 31*, 1464−1476.

Cheng, H. N., & Bovey, F. A. (1977) *Biopolymers 16*, 1465−1472.
Eberhardt, E. S., Loh, S. N., & Raines, R. T. (1993) *Tetrahedron Lett. 34*, 3055−3056.
Engel, J., & Prockop, D. J. (1991) *Annu. Rev. Biophys. Biomol. Struct. 20*, 137−152.
Fischer, G., Bang, H., & Mech, C. (1984) *Biomed. Biochim. Acta 43*, 1101−1111.
Goto, Y., & Hamaguchi, K. (1982) *J. Mol. Biol. 156*, 891−910.
Grathwohl, C., & Wüthrich, K. (1981) *Biopolymers 20*, 2623−2633.
Hagerman, P. J., & Baldwin, R. L. (1976) *Biochemistry 15*, 1462−1473.
Heinemann, U., & Saenger, W. (1982) *Nature 299*, 27−31.
Houry, W. A., Rothwarf, D. M., & Scheraga, H. A. (1994) *Biochemistry 33*, 2516−2530.
Hu, C.-Q., Sturtevant, J. M., Thomson, J. A., Erickson, R. E., & Pace, C. N. (1992) *Biochemistry 31*, 4876−4882.
Jorgensen, W. L., & Gao, J. (1988) *J. Am. Chem. Soc.* 4212−4216.
Kiefhaber, T., & Schmid, F. X. (1992) *J. Mol. Biol. 224*, 231−240.
Kiefhaber, T., Quaas, R., Hahn, U., & Schmid, F. X. (1990a) *Biochemistry 29*, 3053−3061.
Kiefhaber, T., Quaas, R., Hahn, U., & Schmid, F. X. (1990b) *Biochemistry 29*, 3061−3070.
Kiefhaber, T., Grunert, H.-P., Hahn, U., & Schmid, F. X. (1990c) *Biochemistry 29*, 6475−6480.
Kiefhaber, T., Schmid, F. X., Renner, M., & Hinz, H.-J. (1990d) *Biochemistry 29*, 8250−8257.
Kiefhaber, T., Schmid, F. X., Willaert, K., Engelborghs, Y., & Chaffotte, A. (1992a) *Protein Sci. 1*, 1162−1172.
Kiefhaber, T., Kohler, H. H., & Schmid, F. X. (1992b) *J. Mol. Biol. 224*, 217−229.
Lang, K., Schmid, F. X., & Fischer, G. (1987) *Nature 329*, 268−270.
Lin, L.-N., Hasumi, H., & Brandts, J. F. (1988) *Biochim. Biophys. Acta 956*, 256−266.
Martinez-Oyanedel, J., Choe, H.-W., Heinemann, U., & Saenger, W. (1991) *J. Mol. Biol. 222*, 335−352.
Matouschek, A., Rospert, S., Schmid, K., Glick, B. S., & Schatz, G. (1995) *Proc. Natl. Acad. Sci. U.S.A. 92*, 6319−6323.
Mayr, L. M., & Schmid, F. X. (1993a) *Protein Expression Purif. 4*, 52−58.
Mayr, L. M., & Schmid, F. X. (1993b) *J. Mol. Biol. 231*, 913−926.
Mayr, L. M., Kiefhaber, T., & Schmid, F. X. (1993a) in *Protein folding: in vivo and in vitro* (Cleland, J. L., Ed.) pp 142−155, American Chemical Society, Washington.
Mayr, L. M., Landt, O., Hahn, U., & Schmid, F. X. (1993b) *J. Mol. Biol. 231*, 897−912.
Mayr, L. M., Willbold, D., Landt, O., & Schmid, F. X. (1994a) *Protein Sci. 3*, 227−239.
Mayr, L. M., Willbold, D., Rösch, P., & Schmid, F. X. (1994b) *J. Mol. Biol. 240*, 288−293.
Mullins, L. S., Pace, C. N., & Raushel, F. M. (1993) *Biochemistry 32*, 6152−6156.
Mücke, M., & Schmid, F. X. (1994a) *Biochemistry 33*, 12930−12935.
Mücke, M., & Schmid, F. X. (1994b) *Biochemistry 33*, 14608−14619.
Odefey, C., Mayr, L. M., & Schmid, F. X. (1995) *J. Mol. Biol. 245*, 69−78.
Oliveberg, M., Tan, Y.-J., & Fersht, A. R. (1995) *Proc. Natl. Acad. Sci. U.S.A. 92*, 8926−8929.
Pace, C. N., & Laurents, D. V. (1989) *Biochemistry 28*, 2520−2525.
Pace, C. N., Heinemann, U., Hahn, U., & Saenger, W. (1991) *Angew. Chem., Int. Ed. Engl. 30*, 343−360.
Pohl, F. M. (1976) *FEBS Lett. 65*, 293−296.
Privalov, P. L., & Makhatadze, G. I. (1992) *J. Mol. Biol. 224*, 715−723.
Quaas, R., McKeown, Y., Stanssens, P., Frank, R., Blöcker, H., & Hahn, U. (1988) *Eur. J. Biochem. 173*, 617−622.
Ramachandran, G. N., & Mitra, A. K. (1976) *J. Mol. Biol.* 85−92.
Rassow, J., Mohrs, K., Koidl, S., Barthelmess, I. B., Pfanner, N., & Tropschug, M. (1995) *Mol. Cell Biol. 15*, 2654−2662.
Schittkowski, K. (1993) *NLSFIT: a FORTRAN code for parameter estimation in differential equations and explicit model functions*, Universität Bayreuth.
Schmid, F. X. (1986) in *Enzyme Structure, Part L* (Hirs, C. H. W., & Timasheff, S. N., Eds.) pp 71−82, Academic Press, New York.
Schmid, F. X. (1993) *Annu. Rev. Biophys. Biomol. Struct. 22*, 123−143.
Schmid, F. X., & Baldwin, R. L. (1978) *Proc. Natl. Acad. Sci. U.S.A. 75*, 4764−4768.
Schmid, F. X., Mayr, L. M., Mücke, M., & Schönbrunner, E. R. (1993) *Adv. Protein Chem.* 25−66.
Segawa, S.-I., & Sugihara, M. (1984) *Biopolymers 23*, 2473−2488.
Stein, R. L. (1993) *Adv. Protein Chem. 44*, 1−24.
Steinmann, B., Bruckner, P., & Supertifurga, A. (1991) *J. Biol. Chem. 266*, 1299−1303.
Takahashi, K., Uchida, T., & Egami, F. (1970) *Adv. Biophys. 1*, 53−98.
Tonomura, B., Nakatani, H., Ohnishi, M., Yamaguchi-Ito, J., & Hiromi, K. (1978) *Anal. Biochem. 84*, 370−383.
Yu, Y., Makhatadze, G. I., Pace, C. N., & Privalov, P. L. (1994) *Biochemistry 33*, 3312−3319.

BI953035Y